

# Analytical approach to the dynamics of facilitated spin models on random networks

Peter G. Fennell, James P. Gleeson, and Davide Cellai

*MACSI, Department of Mathematics and Statistics, University of Limerick, Ireland*

(Received 23 May 2014; published 30 September 2014)

Facilitated spin models were introduced some decades ago to mimic systems characterized by a glass transition. Recent developments have shown that a class of facilitated spin models is also able to reproduce characteristic signatures of the structural relaxation properties of glass-forming liquids. While the equilibrium phase diagram of these models can be calculated analytically, the dynamics are usually investigated numerically. Here we propose a network-based approach, called approximate master equation (AME), to the dynamics of the Fredrickson-Andersen model. The approach correctly predicts the critical temperature at which the glass transition occurs. We also find excellent agreement between the theory and the numerical simulations for the transient regime, except in close proximity of the liquid-glass transition. Finally, we analytically characterize the critical clusters of the model and show that the departures between our AME approach and the Monte Carlo can be related to the large interface between blocked and unblocked spins at temperatures close to the glass transition.

DOI: [10.1103/PhysRevE.90.032824](https://doi.org/10.1103/PhysRevE.90.032824)

PACS number(s): 64.60.aq, 05.45.-a, 64.70.qj

## I. INTRODUCTION

The nature of the glass transition has been matter of debate for decades. The key point of discussion is whether it is a purely dynamical transition or a manifestation of a genuine thermodynamic amorphous phase (for a review, see, e.g., [1–3]). In order to investigate the first hypothesis, many efforts have been made in defining simple lattice models able to reproduce the fundamental features of the glass transition (see, e.g., [3] and references therein). Among those, facilitated spin models (FSMs), first introduced by Fredrickson and Andersen [4], are perhaps the most classical simple theoretical tool able to reproduce dynamically arrested states. It has become more and more evident, especially in experiments involving colloids, that one of the most important characteristics of glass-forming liquids is the progressive slowing of the dynamics due to the crowding of the space around each particle. Particles spend a long time inside the cage formed by their neighbors and occasionally make a large movement to another cage [5]. A simple way to represent, albeit schematically, this caging effect in a spin model is to prescribe a geometrical constraint that hinders spin flips. Apart from this geometrical constraint, FSMs are characterized by a trivial thermodynamics. Despite the extreme simplicity of these models, recent developments have shown that FSMs are even able to reproduce characteristic signatures of the mode-coupling theory (MCT), one of the most prominent theoretical approaches to glasses [6], including  $A_2$ ,  $A_3$ , and  $A_4$  singularities [7–10].

In spite of the relevance of FSMs, analytical study of these models has usually been focused on the steady state, which can be calculated in simple network topologies [11]. Regarding the dynamics, analytical approaches based on mode-coupling approximations [12,13] and nonequilibrium thermodynamics [14] have been proposed, but they usually struggle in capturing the long-time relaxation of the time correlation function [12,13]. Therefore, most studies strongly rely on Monte Carlo simulations [11,15]. However, numerical simulations become extremely slow in the proximity of the glass transition as the highly constrained kinetics has a direct impact on the speed of Monte Carlo schemes. Therefore, an analytical approach to the dynamics of these models can offer

assistance in understanding the properties of the relaxation process. In this paper, we develop an accurate analytical approximation, named approximate master equation (AME), of the time relaxation of the Fredrickson-Andersen (FA) model. This approach is based on recent work [16], where encapsulating all the nearest neighbor correlations in a master equation provides an extremely powerful tool for a number of binary-state models on random networks, well beyond the mean-field approximation [17]. We extend the master equation approach to the FA model and show that nearest neighbor correlations are sufficient to approximate the dynamics of the model remarkably close to the glass transition. Moreover, we identify critical clusters and show that they are characterized by a large interface between blocked and unblocked spins. This may explain why our approximation of the dynamics deviates from the numerical calculations in the close proximity of the glass transition.

The paper is organized as follows. In Sec. II, we present the FA model. In Sec. III, we describe the AME approach to the FA model and in Sec. IV we compare the results with Monte Carlo simulations. Finally, in Sec. V we analytically characterize the critical clusters of the model and we summarize our conclusions in Sec. VI.

## II. THE FREDRICKSON-ANDERSEN MODEL

The FA model [4] is a spin model where dynamical arrest is entirely driven by a constraint on spin flipping based on the local neighborhood of each node. If we consider that each node  $i$  is either in the state spin-down ( $\sigma_i = -1$ ) or spin-up ( $\sigma_i = +1$ ), the system has Hamiltonian

$$\mathcal{H} = -\frac{1}{2} \sum_i \sigma_i. \quad (1)$$

In addition to this thermodynamically trivial Hamiltonian, there are restrictions on spin flipping. Such restrictions are in the form of a geometric constraint which says that spins can only flip if at least  $f$  of their neighbors are spin-down, where  $f$  is called the facilitation parameter. As a result, a spin on node  $i$  flips at a rate  $W(\sigma_i \rightarrow -\sigma_i) = \min(1, e^{-\sigma_i/T})$ , where

$T$  is the effective temperature of the system, if and only if the condition on the neighborhood is satisfied. This constraint mimics *caging*, a well known feature of glass-forming systems where the movements of molecules or particles, in a material close to dynamical arrest, get progressively restricted in a cage formed by the neighboring particles [5].

For further reference, we can equivalently rewrite the transition rates in order to distinguish the rate  $F(l_i)$  at which a node  $i$  with  $l_i$  spin-down neighbors changes from spin-down to spin-up from  $R(l_i)$ , where the opposite (from spin-up to spin-down) occurs:

$$F(l_i) = \begin{cases} 0 & \text{if } l_i < f, \\ 1 & \text{if } l_i \geq f, \end{cases} \quad (2)$$

$$R(l_i) = \begin{cases} 0 & \text{if } l_i < f, \\ e^{-1/T} & \text{if } l_i \geq f. \end{cases} \quad (3)$$

A relevant quantity in glassy systems is the persistence  $\phi(t)$ . This is the fraction of spins that have never flipped in the time interval  $[0, t]$ . The persistence is a monotonic decreasing function of time whose long time limit,

$$\Phi = \lim_{t \rightarrow \infty} \phi(t), \quad (4)$$

is the fraction of permanently blocked spins and determines whether the system is in a liquid ( $\Phi = 0$ ) or a glass ( $\Phi > 0$ ) state. For large temperature,  $\Phi$  is zero and the system is a liquid. As the temperature decreases, there is a critical temperature  $T_c$  at which  $\Phi$  first becomes nonzero. This is the point of the glass transition. The FA model reproduces this transition, as well as many features related to it, including diverging relaxation times of  $\phi(t)$  close to the critical temperature and dynamical exponents predicted by the MCT [4,7].

On a degree-regular tree graph (Bethe lattice), the FA model can be solved analytically to give an expression for  $\Phi$  as a function of the system temperature  $T$  for fixed facilitation  $f$  [11]. The parameter  $\Phi$  undergoes a discontinuous transition from zero (liquid) to nonzero (glass) at the critical temperature. In this work, we build an analytical framework that gives not only an expression for  $\Phi$ , but also describes the temporal evolution of the persistence,  $\phi(t)$ .

### III. THE FOUR-STATE MASTER EQUATION APPROACH

The AME formalism of [17] has been shown to reproduce a wide range of binary-state dynamics on random networks with great accuracy. The AME is a compartmental model where the dynamics are described by transition rates  $F_{l,m}$  and  $R_{l,m}$  [18], which depend on the number ( $l$  and  $m$ ) of nearest neighbors of a node in each of the two possible states ( $-1$  and  $+1$ ). The FA dynamics are implemented in the AME framework by taking the transition rates to be  $F(l)$  and  $R(l)$ , as given in Eqs. (2) and (3). We show in Appendix A, however, that considering only the spin states of each node (and using therefore a binary AME approach) is not sufficient to capture the complexity of the FA model. Therefore, we extend the AME approach to four-state dynamics by also accounting for the flipping history of each node.

Consider a network with degree distribution  $p_k$  where each node can be in one of four states depending on its spin ( $-1, +1$ ) and whether or not it has previously changed spin

TABLE I. The four possible states in the four-state AME approach. Index refers to the number of neighbors of a node in the corresponding state in the  $\phi_{m_1, m_2, m_3, m_4}^{\pm}$  terminology discussed in the text.

State	Symbol	Spin	History	Index
$(-1, u)$	$\phi^-$	$-1$	Unchanged	$m_1$
$(+1, u)$	$\phi^+$	$+1$	Unchanged	$m_2$
$(-1, c)$	$\psi^-$	$-1$	Changed	$m_3$
$(+1, c)$	$\psi^+$	$+1$	Changed	$m_4$

or is as yet unchanged ( $c, u$ ). These four states are labeled  $(-1, u)$ ,  $(+1, u)$ ,  $(-1, c)$ , and  $(+1, c)$ , as shown in Table I.

Following the FA dynamics, nodes can change from one state to another if the number of their neighbors  $l$  that are in either of the  $(-1, u)$  or  $(-1, c)$  states is at least  $f$ .  $(-1, u)$  nodes will change to  $(+1, c)$  at a rate  $F(l)$ ,  $(+1, u)$  will change to  $(-1, c)$  at a rate  $R(l)$ , and  $(-1, c)$  and  $(+1, c)$  will change back and forth at rates  $F(l)$  and  $R(l)$ , respectively. This is illustrated in Fig. 1.

Given a degree  $k$  and indices  $0 \leq m_i \leq k$  such that  $m_1 + m_2 + m_3 + m_4 = k$ , we define  $\phi_{m_1, m_2, m_3, m_4}^-(t)$  as the fraction of  $k$ -degree nodes in the network that are in state  $(-1, u)$  and which have  $m_1$  neighbors in state  $(-1, u)$ ,  $m_2$  neighbors in state  $(+1, u)$ ,  $m_3$  neighbors in state  $(-1, c)$ , and  $m_4$  neighbors in state  $(+1, c)$  at time  $t$ . The functions  $\phi_{m_1, m_2, m_3, m_4}^+(t)$ ,  $\psi_{m_1, m_2, m_3, m_4}^-(t)$ , and  $\psi_{m_1, m_2, m_3, m_4}^+(t)$  are similarly defined for nodes in states  $(+1, u)$ ,  $(-1, c)$ , and  $(+1, c)$ , respectively. The persistence is then given by

$$\phi(t) = \left\langle \sum_{\vec{m}} [\phi_{m_1, m_2, m_3, m_4}^-(t) + \phi_{m_1, m_2, m_3, m_4}^+(t)] \right\rangle_k, \quad (5)$$

where  $\sum_{\vec{m}}$  is the sum over  $\vec{m}$  with the constraint  $m_1 + m_2 + m_3 + m_4 = k$  and  $\langle \cdot \rangle_k = \sum_{k=0}^{\infty} p_k \cdot$  symbolizes averaging over the degree distribution  $p_k$  of the network.

In the AME, differential equations for the system variables are constructed by considering all flows in and out of compartments. To illustrate, consider an unflipped node in the state  $(-1, u)$  with  $m_1$ ,  $m_2$ ,  $m_3$ , and  $m_4$  neighbors in the states  $(-1, u)$ ,  $(+1, u)$ ,  $(-1, c)$ , and  $(+1, c)$ , respectively. There is a fraction  $\phi_{m_1, m_2, m_3, m_4}^-$  of such nodes in the system. An example of a node of this type with  $m_1 = 2$ ,  $m_2 = 0$ ,  $m_3 = 1$ ,

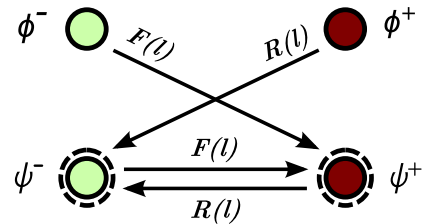


FIG. 1. (Color online) Schematic of the FA dynamics in the four-state approach. The state of a node is a combination of spin-up or spin-down and flipped or unflipped. Here, light green nodes are spin-down and dark red nodes are spin-up, while a dashed circle encompassing the node indicates that it has previously flipped. Nodes change from one state to another according to the transition rates given in Eqs. (2) and (3).

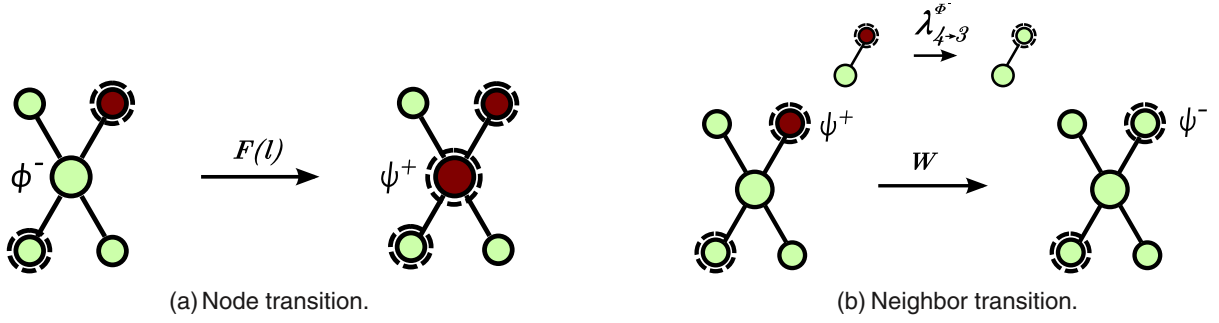


FIG. 2. (Color online) The four-state AME transitions as described in the text. Node transitions are fully specified by the transition rates in Eqs. (2) and (3), while the neighbor transition rates  $W$  are approximated by mean-field transition rates. (a) This unflipped, spin-down node will change state to spin-up at a rate  $F(l)$ , where  $l = m_1 + m_3 = 3$ . (b) The spin-up, changed neighbor of the node will change to spin-down at a rate  $W$  which is approximated by  $\lambda_{4 \rightarrow 3}^{\phi^-}$  as in Eq. (7).

and  $m_4 = 1$  is shown in Figs. 2(a) and 2(b). This node will change to a different class if its state changes from  $(-1, u)$  to  $(+1, c)$  [Fig. 2(a)]. In an infinitesimally small time step  $dt$ , this occurs with probability  $F(m_1 + m_3)dt$ . Thus, the fraction of nodes of this type that will leave the compartment as a result of changing state to  $(+1, c)$  in a small time step  $dt$  is

$$F(m_1 + m_3)\phi_{m_1, m_2, m_3, m_4}^- dt. \quad (6)$$

Similarly, the node will leave the class if one of its neighbors changes state [Fig. 2(b)]. In a time step  $dt$ , one of its  $m_4$  neighbors in the state  $(+1, c)$  will change state to  $(-1, c)$  with probability  $W(\phi_{m_1, m_2, m_3, m_4}^- \rightarrow \phi_{m_1, m_2, m_3+1, m_4-1}^-)dt$ .  $W(\phi_{m_1, m_2, m_3, m_4}^- \rightarrow \phi_{m_1, m_2, m_3+1, m_4-1}^-)$  here is a neighbor transition rate. Unlike the node transition rates  $F$  and  $R$ , the neighbor transition rates are not prespecified. Instead, they are approximated using the time-dependent link transition rates  $\lambda_{i \rightarrow j}^{\phi^-}$  as illustrated in Fig. 2(b). Thus,  $W(\phi_{m_1, m_2, m_3, m_4}^- \rightarrow \phi_{m_1, m_2, m_3+1, m_4-1}^-)$  is approximated by

$$W(\phi_{m_1, m_2, m_3, m_4}^- \rightarrow \phi_{m_1, m_2, m_3+1, m_4-1}^-) \approx m_4 \lambda_{4 \rightarrow 3}^{\phi^-}, \quad (7)$$

where  $\lambda_{4 \rightarrow 3}^{\phi^-}$  is the mean-field rate—determined by averaging over the whole network—at which links of type  $(-1, u)$ —

$(+1, c)$  change to  $(-1, u)$ — $(-1, c)$  and is given by

$$\lambda_{4 \rightarrow 3}^{\phi^-} = \frac{\langle \sum_{\bar{m}} m_1 R(m_1 + m_3) \psi_{m_1, m_2, m_3, m_4}^+ \rangle_k}{\langle \sum_{\bar{m}} m_1 \psi_{m_1, m_2, m_3, m_4}^+ \rangle_k}. \quad (8)$$

The total number of nodes that will leave the class as a result of their neighbors' changing state in a time step  $dt$  is

$$m_1 \lambda_{1 \rightarrow 4}^{\phi^-} \phi_{m_1, m_2, m_3, m_4}^- dt + m_2 \lambda_{2 \rightarrow 3}^{\phi^-} \phi_{m_1, m_2, m_3, m_4}^- dt + m_3 \lambda_{3 \rightarrow 4}^{\phi^-} \phi_{m_1, m_2, m_3, m_4}^- dt + m_4 \lambda_{4 \rightarrow 3}^{\phi^-} \phi_{m_1, m_2, m_3, m_4}^- dt. \quad (9)$$

In the other direction, nodes will enter the class as a result of their neighbors changing state. In a time step  $dt$  the number of these will be

$$(m_1 + 1) \lambda_{1 \rightarrow 4}^{\phi^-} \phi_{m_1+1, m_2, m_3, m_4-1}^- dt + (m_2 + 1) \lambda_{2 \rightarrow 3}^{\phi^-} \phi_{m_1, m_2+1, m_3-1, m_4}^- dt + (m_3 + 1) \lambda_{3 \rightarrow 4}^{\phi^-} \phi_{m_1, m_2, m_3+1, m_4-1}^- dt + (m_4 + 1) \lambda_{4 \rightarrow 3}^{\phi^-} \phi_{m_1, m_2, m_3-1, m_4+1}^- dt. \quad (10)$$

Combining these quantities and taking the limit  $dt \rightarrow 0$  results in the evolution equation for  $\phi_{m_1, m_2, m_3, m_4}^-$ :

$$\begin{aligned} \frac{d}{dt} \phi_{m_1, m_2, m_3, m_4}^- &= -F(m_1 + m_3) \phi_{m_1, m_2, m_3, m_4}^- - m_1 \lambda_{1 \rightarrow 4}^{\phi^-} \phi_{m_1, m_2, m_3, m_4}^- - m_2 \lambda_{2 \rightarrow 3}^{\phi^-} \phi_{m_1, m_2, m_3, m_4}^- - m_3 \lambda_{3 \rightarrow 4}^{\phi^-} \phi_{m_1, m_2, m_3, m_4}^- \\ &\quad - m_4 \lambda_{4 \rightarrow 3}^{\phi^-} \phi_{m_1, m_2, m_3, m_4}^- + (m_1 + 1) \lambda_{1 \rightarrow 4}^{\phi^-} \phi_{m_1+1, m_2, m_3, m_4-1}^- + (m_2 + 1) \lambda_{2 \rightarrow 3}^{\phi^-} \phi_{m_1, m_2+1, m_3-1, m_4}^- \\ &\quad + (m_3 + 1) \lambda_{3 \rightarrow 4}^{\phi^-} \phi_{m_1, m_2, m_3+1, m_4-1}^- + (m_4 + 1) \lambda_{4 \rightarrow 3}^{\phi^-} \phi_{m_1, m_2, m_3-1, m_4+1}^-. \end{aligned} \quad (11)$$

A similar equation can be written for  $\phi_{m_1, m_2, m_3, m_4}^+$ . The evolution equations for  $\psi_{m_1, m_2, m_3, m_4}^-$  and  $\psi_{m_1, m_2, m_3, m_4}^+$  differ as they include nodes who enter the class as a result of changing state; for example this extra term for the  $\psi_{m_1, m_2, m_3, m_4}^-$  variable is

$$R(m_1 + m_3) \phi_{m_1, m_2, m_3, m_4}^+ + R(m_1 + m_3) \psi_{m_1, m_2, m_3, m_4}^+. \quad (12)$$

The full set of equations are given in Appendix B. The initial conditions of this set of equations are the following. At time

$t = 0$ , no nodes will have flipped and so

$$\psi_{m_1, m_2, m_3, m_4}^-(0) = \psi_{m_1, m_2, m_3, m_4}^+(0) = 0 \quad (13)$$

for all values  $m_1, m_2, m_3, m_4$  and

$$\phi_{m_1, m_2, m_3, m_4}^-(0) = \phi_{m_1, m_2, m_3, m_4}^+(0) = 0, \quad (14)$$

when  $m_3 > 0$  or  $m_4 > 0$ . Furthermore, for the FA system with temperature  $T$  there is a fraction  $\rho = 1/(1 + e^{-1/T})$  of spin-up nodes at thermal equilibrium. This gives the initial conditions on the unflipped variables for which  $m_3 = m_4 = 0$ :

$$\phi_{m_1, m_2, 0, 0}^-(0) = p_k (1 - \rho) \binom{k}{m_1} (1 - \rho)^{m_1} \rho^{m_2}, \quad (15)$$

$$\phi_{m_1, m_2, 0, 0}^+(0) = p_k \rho \binom{k}{m_1} (1 - \rho)^{m_1} \rho^{m_2}. \quad (16)$$

The master equations hold for all  $m_1 + m_2 + m_3 + m_4 = k$  and for all values of  $k$ , resulting in a closed system of deterministic equations from which the expression for the evolution of the persistence is obtained:

$$\begin{aligned} \frac{d\phi}{dt} &= \left\langle \sum_{\vec{m}} \left( \frac{d}{dt} \phi_{m_1, m_2, m_3, m_4}^- + \frac{d}{dt} \phi_{m_1, m_2, m_3, m_4}^+ \right) \right\rangle_k \\ &= - \left\langle \sum_{\vec{m}} [F(m_1 + m_3) \phi_{m_1, m_2, m_3, m_4}^- \right. \\ &\quad \left. + R(m_1 + m_3) \phi_{m_1, m_2, m_3, m_4}^+] \right\rangle_k. \end{aligned} \quad (17)$$

The solution of the steady state is obtained by setting  $d\phi/dt$  in Eq. (17), and all the time derivatives of  $\phi_{m_1, m_2, m_3, m_4}^-$  and  $\phi_{m_1, m_2, m_3, m_4}^+$  in Eqs. (11) and (B2), equal to zero.

Unlike the binary-state case (see Appendix A), the four-state AME captures the complexities of the FA models. In the next section, we show that the value of  $\Phi$  predicted by the AME corresponds to the value of  $\Phi$  given calculated by Monte Carlo (MC) simulations of the FA model. Furthermore, the evolution of  $\phi(t)$  in the MC simulations is matched well by the AME, with the only discrepancies arising in the late relaxation of  $\phi(t)$  for temperatures close to the glass transition. In the final section, we explore the AME system of equations to explain this discrepancy and gain an insight into the mechanism by which the system gets stuck in the glassy state.

## IV. RESULTS

### A. Steady states

The steady states ( $t \rightarrow \infty$ ) of the FA model can be calculated analytically [11]. Here we reproduce the derivation for further reference. For the sake of clarity, in the following calculations we consider a degree-regular graph. However, the extension to a locally treelike network with a generic degree distribution  $p_k$  (also called ‘‘configuration model’’) is straightforward. This approach is valid as in the configuration model the density of finite cycles vanishes as the network size diverges. Let  $\rho = 1/(1 + e^{-1/T})$  be the fraction of spin-up nodes at thermal equilibrium, as in Sec. III. Let us define  $Z_{++}$  and  $Z_{-+}$  as the probability that, following an edge starting from a  $\sigma = +1$  (respectively,  $\sigma = -1$ ) spin, we get to a  $\phi^+$  node, i.e., a node with  $\sigma = +1$  spin which belongs to a cluster of blocked spins. Then the following equations hold:

$$Z_{++} = \rho \sum_{l=k-f}^{k-1} \binom{k-1}{l} (Z_{++})^l (1 - Z_{++})^{k-1-l}, \quad (18)$$

$$Z_{-+} = \rho \sum_{l=k-f+1}^{k-1} \binom{k-1}{l} (Z_{++})^l (1 - Z_{++})^{k-1-l}. \quad (19)$$

In Eq. (18), the right-hand side calculates all the possibilities of having at least  $(k - f)$  outgoing  $\phi^+$  neighbors. The sum in (19) starts from  $(k - f + 1)$ , instead, because on the other end point of the considered edge there is a  $\sigma = -1$  spin; thus, only  $(k - f)$  outgoing  $\phi^+$  neighbors would not be enough to guarantee the blockage of the considered node. We also note that  $Z_{-+}$  is just a function of  $Z_{++}$ . The total fraction of blocked spins is then

$$\Phi = \Phi^+ + \Phi^-, \quad (20)$$

where

$$\Phi^+ = \rho \sum_{l=k-f+1}^k \binom{k}{l} (Z_{++})^l (1 - Z_{++})^{k-l}, \quad (21)$$

$$\Phi^- = (1 - \rho) \sum_{l=k-f+1}^k \binom{k}{l} (Z_{-+})^l (1 - Z_{-+})^{k-l}. \quad (22)$$

Equation (18) has the same form of the corresponding equation for  $k$ -core percolation [19] and it has been shown [11,19] that the position of the phase transition can be calculated by imposing the conditions

$$\begin{cases} g(Z_{++}) = 1, \\ g'(Z_{++}) = 0, \end{cases} \quad (23)$$

where

$$g(Z_{++}) = \rho \sum_{l=k-f}^{k-1} \binom{k-1}{l} (Z_{++})^{l-1} (1 - Z_{++})^{k-1-l}. \quad (24)$$

To allow for comparison with previous results [7,11], we now consider a degree-regular graph with  $k = 4$  ( $p_k = \delta_{k,4}$ ) and facilitation parameter  $f = 2$ . Solving Eq. (23), one can find a transition point  $\rho_c = 8/9$ , which corresponds to the critical temperature  $T_c = 1/\ln(8) = 0.480898$ . Figure 3 shows the behavior of  $\Phi$  at different temperatures. At  $T > T_c$ , the system can relax completely after a transient regime and

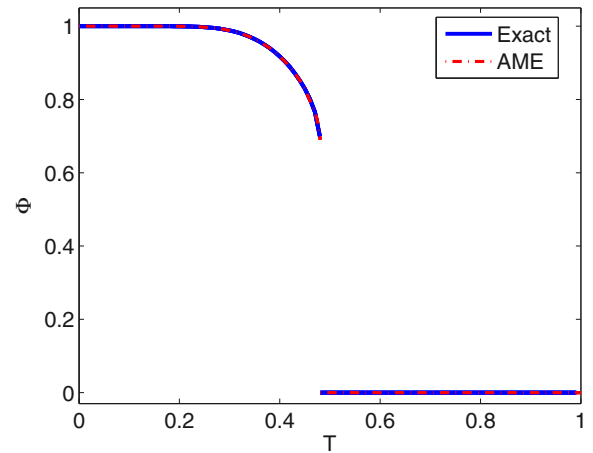


FIG. 3. (Color online) Fraction of blocked spins  $\Phi$  as a function of the temperature  $T$ . The blue solid line is the analytical calculation of the steady state as given by Eq. (23), while the red dash-dotted line is calculated by our AME approach. It is evident that the AME predicts the exact steady state, and thus the critical temperature  $T_c$ , very accurately.



there are no blocked spins in the limit  $t \rightarrow \infty$ . At  $T < T_c$ , a finite fraction of spins remains blocked even after an infinite time. The transition between the two phases is discontinuous with a hybrid nature as this model is in the same universality class as bootstrap and  $k$ -core percolation models [19–21].

The exact value of  $\Phi$  as given by Eq. (20) is compared with the steady-state values of our AME method in Fig. 3. It can be seen that the AME reproduces the (known) steady state almost exactly, even in the proximity of the glass transition. An implication of this is that the AME predicts the critical temperature  $T_c$  exactly.

### B. Dynamics

We now turn to the dynamics of the FA model and compare the results of calculations from our AME approach to MC simulations. The MC simulations are carried out on a configuration model network, a random network entirely described by its degree distribution  $p_k$ . The network consists of  $N = 2^{18}$  nodes and is updated asynchronously using a time step of  $dt = 1/N$ . The simulations are carried out in C/C++. The numerical integration of the AME are carried out in MATLAB/OCTAVE [22]. As in the case of the steady state, we consider a degree-regular graph with  $k = 4$  ( $p_k = \delta_{k,4}$ ) and facilitation parameter  $f = 2$ . Because of the presence of the discontinuous transition, we expect this case to be more challenging for our approximation with respect to other parameter choices where the transition is instead continuous.

We consider various values of  $T$  above and below the critical temperature  $T_c$ . Figure 4 shows the evolution of the persistence  $\phi(t)$  for both the AME and the MC simulations. Overall, we see that the AME matches the MC simulations quite well in the transient regime. At high temperatures, the geometric constraint is less important and a detailed computation of short-ranged correlations is sufficient to capture the overall behavior of the persistence  $\phi(t)$ .

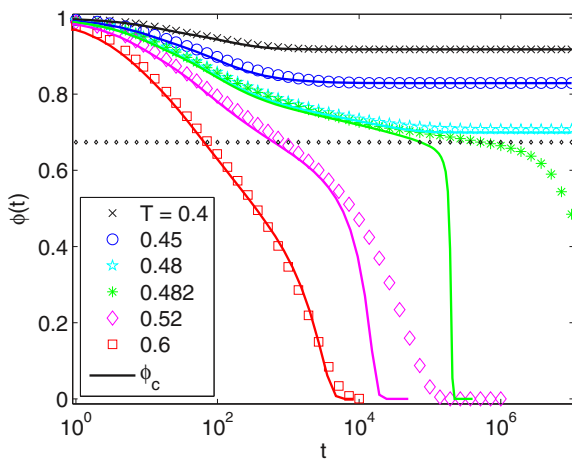


FIG. 4. (Color online) Time evolution of the fraction of unflipped spins  $\phi(t)$  for different values of the temperature  $T$  with facilitation parameter  $f = 2$ . Symbols are MC simulations over 4-regular graphs (Bethe lattice) of size  $N = 2^{18}$ , averaged over 12 realizations. Continuous lines are calculated with the AME approach. The dotted line corresponds to the critical value of blocked spins  $\Phi_c \simeq 0.69$ .

In the proximity of the glass transition, at  $T \gtrsim T_c$ , the transient regime can be characterized by a two-step relaxation form where the two steps are the approach and departure from the critical plateau. These are called the  $\beta$ - and  $\alpha$ -relaxation regimes, respectively [1]. The long-ranged correlations typical of the glass transition at this temperature range cannot be reproduced by our AME approach, but they become more and more important closer to the transition. Therefore, we see the AME prediction of the  $\alpha$ -relaxation regime become significantly less accurate as we approach the transition, despite the fact that both the  $\beta$ -relaxation regime and steady states are correctly reproduced as seen in Figs. 4 and 3, respectively.

At  $T < T_c$ , there is excellent agreement between theory and simulations with the analytic curve reaching the exact steady state. In this regime, it transpires, our approximation improves again as a large portion of the network remains blocked and therefore the error in describing the arrangements of flipping spins has a smaller effect. It can be shown that our numerical results are robust against finite size analysis.

To investigate more carefully the differences between our AME approach and the MC simulations on approaching the transition, we analyze the local arrangements of spins in the steady state. This is achieved by equating the derivative of  $\phi(t)$  in Eq. (17) to zero and exploring this and the master equations to see the possible system configurations under which a nonzero value of  $\Phi$  is possible.

It is evident that  $\phi$  will be in the steady state only if each of the  $\phi_{m_1, m_2, m_3, m_4}^-$  and  $\phi_{m_1, m_2, m_3, m_4}^+$  variables are also in the steady state. However, there are no requirements for the  $\psi_{m_1, m_2, m_3, m_4}^-$  and  $\psi_{m_1, m_2, m_3, m_4}^+$  variables to be in a steady state, and indeed one of the configurations of the system at equilibrium is a dynamical one where the flipped nodes are still mobile and dynamically active. The system configuration in this regime is summarized in Table II.

The other possible configuration of the system at equilibrium is one where every node is immobile, being surrounded by less than  $f$  spin-down nodes. However, this configuration is highly unlikely for nonzero values of  $T$  and furthermore it is not observed in the numerical simulations; we henceforth only regard the dynamical steady state.

Analysis of the steady-state equations for the dynamical equilibrium yields the following conditions. The first is that

$$\bar{\phi}_{m_1, m_2, m_3, m_4}^+ = \bar{\phi}_{m_1, m_2, m_3, m_4}^- = 0 \quad \forall m_1 + m_3 \geq f. \quad (25)$$

TABLE II. The only values of  $m_1$ ,  $m_2$ ,  $m_3$ , and  $m_4$  for which the different AME variables are nonzero in the dynamical steady-state regime. Overbars denotes the steady-state value.

Nonzero variables	
$\bar{\phi}_{m_1, m_2, m_3, m_4}^-$	$m_3 = m_4 = 0$ and $m_1 + m_3 < f$
$\bar{\phi}_{m_1, m_2, m_3, m_4}^+$	$m_3 = m_4 = 0$ and $m_1 + m_3 < f$
$\bar{\psi}_{m_1, m_2, m_3, m_4}^-$	$m_1 = m_2 = 0$
$\bar{\psi}_{m_1, m_2, m_3, m_4}^+$	$m_1 = m_2 = 0$

This simply states that the unflipped nodes can remain in the system but only if they are surrounded by less than  $f$  spin-down nodes and so are immobile. The second condition is on the neighbor transition rate approximations. This condition is that all of these rates are zero except for  $\lambda_{3 \rightarrow 4}^{\psi^-}$ ,  $\lambda_{4 \rightarrow 3}^{\psi^-}$ ,  $\lambda_{3 \rightarrow 4}^{\psi^+}$ , and  $\lambda_{4 \rightarrow 3}^{\psi^+}$ . These four rates describe the transitions of flipped neighbors of flipped nodes. The fact that they are nonzero in the steady-state regime of  $\phi$ , while the other transition rates are zero, indicates that the four-state AME approach recreates dynamical heterogeneity, a stylized fact of the glass transition [2] where blocked nodes and mobile nodes can coexist when the system is in dynamical equilibrium.

The neighbor transition rates are functions of the state variables as shown in Eq. (8), and so for the transition rates to satisfy the second condition it is required that

$$\bar{\phi}_{m_1, m_2, m_3, m_4}^- = \bar{\phi}_{m_1, m_2, m_3, m_4}^+ = 0 \quad \forall m_3, m_4 > 0, \quad (26)$$

$$\bar{\psi}_{m_1, m_2, m_3, m_4}^- = \bar{\psi}_{m_1, m_2, m_3, m_4}^+ = 0 \quad \forall m_1, m_2 > 0. \quad (27)$$

This implies that there are no links between changed and unchanged nodes. The reason that this condition is necessary is because of the neighbor transition rate approximation. This is illustrated in Fig. 5, where we show the two types of node-neighbor configurations that can appear at the boundary and are observed in the MC simulations. Note that, in reality, the flipped neighbor of the central node in Fig. 5(a) will be able to flip without releasing the cluster because the node has no other spin-down neighbors. However, the flipped neighbor of the node in Fig. 5(b) will not be able to flip without releasing the cluster, because if it flips to spin-down then the node will have sufficiently many spin-down neighbors to flip. Therefore, in reality, the neighbor transition rate  $W(\phi_{0,3,0,1}^+ \rightarrow \phi_{0,3,1,0}^+)$  for the node in Fig. 5(a) should be nonzero while the neighbor transition rate  $W(\phi_{1,2,0,1}^+ \rightarrow \phi_{1,2,1,0}^+)$  in Fig. 5(b) should be zero. However, the AME approximates neighbor transitions

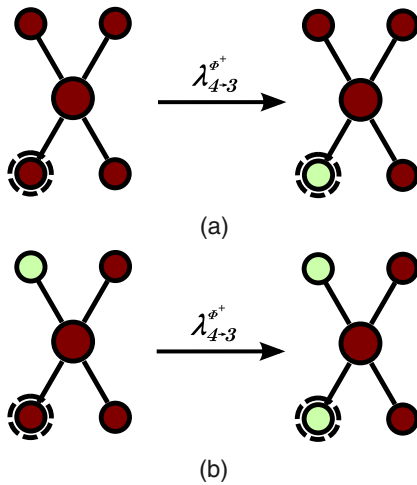


FIG. 5. (Color online) (a) Example of a blocked spin at the interface which remains blocked regardless of its  $\phi^+$  neighbor flipping. (b) Example of a blocked spin at the interface which becomes flippable after the change of its  $\phi^+$  neighbor. Here the facilitation parameter is  $f = 2$ . In the AME, the two transition rates as shown by (a) and (b) here are the same as they are both approximated by  $\lambda_{4 \rightarrow 3}^{\phi^+}$ .

by link transitions, and in this case the two transition rates are approximated by the same link transition rate  $\lambda_{4 \rightarrow 3}^{\phi^+}$ . This link transition rate is necessarily zero to prevent the release of the nodes of type Fig. 5(b). However, this link transition rate is of the form of Eq. (8), and for its value to be zero it is required that links of this type do not exist.

Thus, the approximation of the neighbor transition rates by the AME is compensated by the assumption that the size of boundary between the blocked and mobile clusters is zero. It will be now shown that it is this zero-boundary assumption that causes the inaccuracy of the AME in the  $\alpha$ -relaxation regime as the size of the boundary, or, in fact, the size of the critical clusters with large interface that compose it, diverges on approaching the glass transition.

## V. CRITICAL CLUSTERS

Progress in approaching analytically the equilibrium properties of the FA model has been quite slow. It took about 20 y, since the introduction of the model, for the steady states to be calculated on a locally treelike network [11]. Here we show that it is also possible to characterize the critical clusters of the FA model by using a formalism recently developed in network percolation. It has been noted [23] that the FA model is very similar to  $k$ -core percolation and therefore the critical clusters of the FA model should correspond to the so-called corona clusters in  $k$ -core percolation [24]. However, the FA model is slightly more complex than  $k$ -core percolation and, to the best of our knowledge, it has not been shown explicitly that the critical clusters of the FA model can indeed be calculated following the same procedure used for  $k$ -core percolation. In this section we give a definition of critical clusters as a subset of the blocked clusters in the steady state and analytically prove that their mean size diverges at the phase transition. As the found critical clusters are characterized by a large number of interface edges, this also explains why the quality of our AME approximation deteriorates at the phase transition.

In analogy with the corona clusters in  $k$ -core percolation [24], we now consider as critical clusters the subsets of the blocked clusters where the minimum local requirement is exactly satisfied for all the nodes in the critical cluster. In other words, a node belongs to such clusters if it is in a blocked cluster and it has exactly  $(k - f + 1) \phi^+$  neighbors: The flipping of just one of the  $\phi^+$ -neighboring spins would create a cascade of movements that would eventually destroy the whole considered critical cluster at  $t \rightarrow \infty$ . Our goal is to prove that these clusters are critical by showing that their mean size diverges at the transition. In order to do that, we use the generating function formalism as in [24,25]. We define  $H_{++}(x)$  as the generating function of the probability that, following an edge in a blocked cluster from a  $(\sigma = +1)$ -spin, one gets to a spin  $\sigma = +1$  node, which belongs to a finite critical cluster. Similarly, we define  $H_{-+}(x)$  as the generating function of the probability that, following an edge in a blocked cluster from a  $(\sigma = -1)$  spin, one gets to a spin  $\sigma = +1$  node, which belongs to a finite critical cluster. Then, the following equation holds:

$$H_{++}(x) = Q_{++} + xG_{++}[H_{++}(x)], \quad (28)$$

where

$$Q_{++} = \rho \sum_{l=k-f+1}^{k-1} \binom{k-1}{l} (Z_{++})^l (1-Z_{++})^{k-1-l}, \quad (29)$$

$$G_{++}(x) = \rho \binom{k-1}{k-f} (1-Z_{++})^{f-1} x^{k-f}. \quad (30)$$

Accordingly,  $Q_{++}$  represents the probability that, following an edge in a blocked cluster, one gets to a  $\phi^+$  node which does not belong to a critical cluster because it has at least  $(k-f+1)$   $\phi^+$  neighbors (so more than the minimum requirement), while  $G_{++}(x)$  calculates the number of ways the  $\phi^+$  edge end point can have exactly  $(k-f)$  potential  $\phi^+$  neighbors. It is easy to notice that  $G_{++}(Z_{++}) = Z_{++} - Q_{++}$  and  $H_{++}(1) = Z_{++}$ . An analogous equation can be written for  $H_{-+}(x)$ . The generating function  $H_0(x)$  of the critical cluster sizes is then given by

$$H_0(x) = \sum_{l=k-f+1}^k \{P_+(l)[H_{++}(x)]^l + P_-(l)[H_{-+}(x)]^l\}, \quad (31)$$

where

$$P_+(l) = \frac{\rho \binom{k}{l} (Z_{++})^l (1-Z_{++})^{k-l}}{\Phi_+}, \quad (32)$$

$$P_-(l) = \frac{(1-\rho) \binom{k}{l} (Z_{-+})^l (1-Z_{-+})^{k-l}}{\Phi_-}, \quad (33)$$

are the degree distributions in blocked clusters for nodes with spins up and down, respectively.

The mean size of the critical clusters is given by  $H'_0(1)$ , which, being a linear combination of  $H_{++}(1)$  and  $H_{-+}(1)$ , diverges at the phase transition only if the latter quantities do. Therefore, as we have seen that  $H_{++}(1) = Z_{++}$ , we concentrate now on calculating  $H'_{++}(1)$ . From (28), we get

$$H'_{++}(1) = \frac{Z_{++} - Q_{++}}{1 - G'_{++}(Z_{++})}. \quad (34)$$

From the second condition of criticality (23) and Eq. (30) we obtain

$$\begin{aligned} \rho \sum_{l=k-f}^{k-2} \binom{k-1}{l+1} (Z_{++})^l (1-Z_{++})^{k-l-2} \\ = \frac{k-f-1}{k-f} G'(Z_{++}), \end{aligned} \quad (35)$$

from which

$$\begin{aligned} g(Z_{++}) = \frac{G'(Z_{++})}{k-f} + \rho \sum_{l=k-f}^{k-2} \binom{k-1}{l+1} \\ \times (Z_{++})^l (1-Z_{++})^{k-l-2} = G'(Z_{++}). \end{aligned} \quad (36)$$

Then, from the first condition of criticality (23) we have  $g(Z_{++}) = G'_{++}(Z_{++}) = 1$ . Therefore, we have proved analytically that the investigated clusters are, indeed, critical, because at the phase transition their mean size diverges according to (34).

## VI. CONCLUSIONS

In this paper, we have introduced analytical approaches to investigate both the steady state and the time relaxation of the FA model. Our analysis has then been compared with numerical simulations. We have extended to a four-state model an AME formalism [17] to reproduce the dynamics of the model. Unlike earlier theoretical approaches, our formalism is able to reproduce both the exact steady state and the transient regime. In particular, we show that our approximation can partially capture dynamical heterogeneity, a characteristic of glassy systems where mobile and blocked clusters coexist. The degree of accuracy of the analytical approximation compared to the MC is excellent, in general, save for a range of temperatures close to the critical temperature. We identify as a source of error the difficulty for the AME in capturing boundaries between blocked and flippable clusters. To properly investigate this issue, we analytically identify the critical clusters of the model and show that at the glass transition the interface dominates the blocked clusters. Therefore, also at  $T \gtrsim T_c$  the dynamics should be largely affected by the slow unblocking of large quasicritical clusters, with many interface edges that are not exactly captured by the AME.

There is much scope for progress in investigating this type of glass model using our four-state AME approach. Here the model was implemented on a degree-regular network where each node had the same facilitation  $f = 2$ . Richer behavior occurs if the facilitation parameter value is allowed to vary between nodes [7]. In this framework, this is equivalent to considering a model with uniform  $f$  but where nodes do not all have the same degree. In other words, an appropriate definition of the degree distribution determines the model one may wish to study. Degree variation in the four-state AME formalism can be naturally implemented through the degree distribution  $p_k$ . Moreover, it is straightforward to extend the formalism we use to calculate the critical clusters in a network with a given degree distribution.

This work also paves the way for further analytical exploration of the model. An expression for  $\Phi$  can be obtained by taking the pair approximation to the full system of master equations [17]. Generating functions can be used to reduce the system of master equation to a set of ordinary differential equations [26]. Finally, MCT makes predictions about the temporal evolution of glassy systems such as relationships between relaxation time exponents. While the past study of this area was restricted to examination of the MC simulations, our formalism may give scope for analytical investigations.

## ACKNOWLEDGMENTS

This work has been partially funded by Science Foundation Ireland, Grant No. 11/PI/1026, and the FET-Proactive project PLEXMATH (FP7-ICT-2011-8; Grant No. 317614), funded by the European Commission. We acknowledge the DJEI/DES/SFI/HEA Irish Centre for High-End Computing (ICHEC) for the provision of computational facilities and support.

**APPENDIX A: BINARY-STATE APPROACH**

For the binary-state approach, we only distinguish the spin state of nodes. Therefore, the model variables are  $\phi_{l,m}^-$  and  $\phi_{l,m}^+$ , the fraction of  $-1$  (respectively  $+1$ ) nodes in the network which have not previously flipped and which have  $l$  neighbors in the state  $-1$  and  $m$  neighbors in the state  $+1$ , for all values  $l + m = k$  for all possible  $k$ . In the same manner as described in Sec. III, master equations for  $\phi_{l,m}^-$  and  $\phi_{l,m}^+$  can be constructed. The evolution equation for  $\phi_{l,m}^-$ , before approximation of the neighbor transition rates as in Eq. (7) in the four-state case, is given by

$$\begin{aligned} \frac{d}{dt}\phi_{l,m}^- &= -F(l)\phi_{l,m}^- - W(\phi_{l,m}^- \rightarrow \phi_{l+1,m-1}^-)\phi_{l,m}^- \\ &\quad - W(\phi_{l,m}^- \rightarrow \phi_{l-1,m+1}^-)\phi_{l,m}^- \\ &\quad + W(\phi_{l+1,m-1}^- \rightarrow \phi_{l,m}^-)\phi_{l+1,m-1}^- \\ &\quad + W(\phi_{l-1,m+1}^- \rightarrow \phi_{l,m}^-)\phi_{l-1,m+1}^-, \end{aligned} \quad (\text{A1})$$

with a similar equation for  $\phi_{l,m}^+$ . The evolution of the persistence is then simply

$$\begin{aligned} \frac{d}{dt}\Phi &= \left\langle \sum_{l=0}^k \frac{d}{dt}\phi_{l,m}^- + \frac{d}{dt}\phi_{l,m}^+ \right\rangle_k \\ &= - \left\langle \sum_{l=0}^k F(l)\phi_{l,m}^- + R(l)\phi_{l,m}^+ \right\rangle_k. \end{aligned} \quad (\text{A2})$$

Equation (A2), along with the system of differential equations for  $\phi_{l,m}^-$  and  $\phi_{l,m}^+$  as given by Eq. (A1), can be equated to zero to solve for conditions yielding a nonzero value of  $\Phi$  and thus the glassy state. The steady-state solution to Eq. (A2) gives the condition that  $\phi_{l,m}^-$  is zero for  $l \geq f$  and nonzero for  $l < f$ , with the same condition for  $\phi_{l,m}^+$ . This is obvious, implying that unflipped nodes can remain in the system but

only if they are surrounded by at most  $f - 1$  spin-down nodes.

Of more interest are the conditions on the neighbor transition rates which arise from the steady-state solutions to the differential equations for  $\phi_{l,m}^-$  and  $\phi_{l,m}^+$ . These conditions are that

$$\begin{aligned} W(\phi_{l,m}^- \rightarrow \phi_{l+1,m-1}^-) &\begin{cases} >0 & 0 \leq l < f-1, \\ =0 & f-1 \leq l < k, \end{cases} \\ W(\phi_{l,m}^- \rightarrow \phi_{l-1,m+1}^-) &\begin{cases} >0 & 0 < l \leq f-1, \\ =0 & f-1 < l \leq k, \end{cases} \end{aligned} \quad (\text{A3})$$

with the same conditions for  $W(\phi_{l,m}^+ \rightarrow \phi_{l+1,m-1}^+)$  and  $W(\phi_{l,m}^+ \rightarrow \phi_{l-1,m+1}^+)$ .

As mentioned earlier, the neighbor transition rates of the AME are not exact but rather approximated by mean-field link transition rates [17]. For example, the second transition rate in Eq. (A1) is approximated by

$$W(\phi_{l,m}^- \rightarrow \phi_{l-1,m+1}^-) \approx l\beta^-, \quad (\text{A4})$$

where  $\beta^-$  is the mean-field rate that a link of type  $(-1)-(-1)$  changes to  $(-1)-(+1)$  and is given by

$$\beta^- = \frac{\left\langle \sum_{l=0}^k l F(l) \phi_{l,m}^- \right\rangle_k}{\left\langle \sum_{l=0}^k l \phi_{l,m}^- \right\rangle_k}, \quad (\text{A5})$$

see [17] for details. This is the level of approximation in the model. These mean-field rates fail to capture the dynamic heterogeneities of the FA system. In particular, they are always nonzero and so do not satisfy the neighbor transition rate condition of Eq. (A3). This implies that a nonzero value of  $\Phi$  is impossible in the binary-state AME for all values of the temperature  $T$  and so  $\Phi \equiv 0$ . This is not accurate, as the exact value of  $\Phi$  is nonzero for all  $T < T_c$ , as can be seen in Fig. 3, and so we conclude that a binary-state AME—accounting only for the spin of each node—is not sufficient to capture the FA model.

**APPENDIX B: FULL SET OF EQUATIONS**

The full set of equations for the four-state AME, as described in Sec. III, is given by

$$\begin{aligned} \frac{d}{dt}\phi_{m_1,m_2,m_3,m_4}^- &= -F(m_1 + m_3)\phi_{m_1,m_2,m_3,m_4}^- - m_1\lambda_{1 \rightarrow 4}^{\phi^-}\phi_{m_1,m_2,m_3,m_4}^- - m_2\lambda_{2 \rightarrow 3}^{\phi^-}\phi_{m_1,m_2,m_3,m_4}^- - m_3\lambda_{3 \rightarrow 4}^{\phi^-}\phi_{m_1,m_2,m_3,m_4}^- \\ &\quad - m_4\lambda_{4 \rightarrow 3}^{\phi^-}\phi_{m_1,m_2,m_3,m_4}^- + (m_1 + 1)\lambda_{1 \rightarrow 4}^{\phi^-}\phi_{m_1+1,m_2,m_3,m_4-1}^- + (m_2 + 1)\lambda_{2 \rightarrow 3}^{\phi^-}\phi_{m_1,m_2+1,m_3-1,m_4}^- \\ &\quad + (m_3 + 1)\lambda_{3 \rightarrow 4}^{\phi^-}\phi_{m_1,m_2,m_3+1,m_4-1}^- + (m_4 + 1)\lambda_{4 \rightarrow 3}^{\phi^-}\phi_{m_1,m_2,m_3-1,m_4+1}^-, \end{aligned} \quad (\text{B1})$$

$$\begin{aligned} \frac{d}{dt}\phi_{m_1,m_2,m_3,m_4}^+ &= -R(m_1 + m_3)\phi_{m_1,m_2,m_3,m_4}^+ - m_1\lambda_{1 \rightarrow 4}^{\phi^+}\phi_{m_1,m_2,m_3,m_4}^+ - m_2\lambda_{2 \rightarrow 3}^{\phi^+}\phi_{m_1,m_2,m_3,m_4}^+ - m_3\lambda_{3 \rightarrow 4}^{\phi^+}\phi_{m_1,m_2,m_3,m_4}^+ \\ &\quad - m_4\lambda_{4 \rightarrow 3}^{\phi^+}\phi_{m_1,m_2,m_3,m_4}^+ + (m_1 + 1)\lambda_{1 \rightarrow 4}^{\phi^+}\phi_{m_1+1,m_2,m_3,m_4-1}^+ + (m_2 + 1)\lambda_{2 \rightarrow 3}^{\phi^+}\phi_{m_1,m_2+1,m_3-1,m_4}^+ \\ &\quad + (m_3 + 1)\lambda_{3 \rightarrow 4}^{\phi^+}\phi_{m_1,m_2,m_3+1,m_4-1}^+ + (m_4 + 1)\lambda_{4 \rightarrow 3}^{\phi^+}\phi_{m_1,m_2,m_3-1,m_4+1}^+, \end{aligned} \quad (\text{B2})$$

$$\begin{aligned} \frac{d}{dt}\psi_{m_1,m_2,m_3,m_4}^- &= -F(m_1 + m_3)\psi_{m_1,m_2,m_3,m_4}^- + R(m_1 + m_3)\phi_{m_1,m_2,m_3,m_4}^+ + R(m_1 + m_3)\psi_{m_1,m_2,m_3,m_4}^+ - m_1\lambda_{1 \rightarrow 4}^{\psi^-}\psi_{m_1,m_2,m_3,m_4}^- \\ &\quad - m_2\lambda_{2 \rightarrow 3}^{\psi^-}\psi_{m_1,m_2,m_3,m_4}^- - m_3\lambda_{3 \rightarrow 4}^{\psi^-}\psi_{m_1,m_2,m_3,m_4}^- - m_4\lambda_{4 \rightarrow 3}^{\psi^-}\psi_{m_1,m_2,m_3,m_4}^- + (m_1 + 1)\lambda_{1 \rightarrow 4}^{\psi^-}\psi_{m_1+1,m_2,m_3,m_4-1}^- \\ &\quad + (m_2 + 1)\lambda_{2 \rightarrow 3}^{\psi^-}\psi_{m_1,m_2+1,m_3-1,m_4}^- + (m_3 + 1)\lambda_{3 \rightarrow 4}^{\psi^-}\psi_{m_1,m_2,m_3+1,m_4-1}^- + (m_4 + 1)\lambda_{4 \rightarrow 3}^{\psi^-}\psi_{m_1,m_2,m_3-1,m_4+1}^-, \end{aligned} \quad (\text{B3})$$



$$\begin{aligned} \frac{d}{dt} \psi_{m_1, m_2, m_3, m_4}^+ = & -R(m_1 + m_3) \psi_{m_1, m_2, m_3, m_4}^+ + F(m_1 + m_3) \phi_{m_1, m_2, m_3, m_4}^- + F(m_1 + m_3) \psi_{m_1, m_2, m_3, m_4}^- - m_1 \lambda_{1 \rightarrow 4}^{\psi^+} \psi_{m_1, m_2, m_3, m_4}^+ \\ & - m_2 \lambda_{2 \rightarrow 3}^{\psi^+} \psi_{m_1, m_2, m_3, m_4}^+ - m_3 \lambda_{3 \rightarrow 4}^{\psi^+} \psi_{m_1, m_2, m_3, m_4}^+ - m_4 \lambda_{4 \rightarrow 3}^{\psi^+} \psi_{m_1, m_2, m_3, m_4}^+ + (m_1 + 1) \lambda_{1 \rightarrow 4}^{\psi^+} \psi_{m_1+1, m_2, m_3, m_4-1}^+ \\ & + (m_2 + 1) \lambda_{2 \rightarrow 3}^{\psi^+} \psi_{m_1, m_2+1, m_3-1, m_4}^+ + (m_3 + 1) \lambda_{3 \rightarrow 4}^{\psi^+} \psi_{m_1, m_2, m_3+1, m_4-1}^+ + (m_4 + 1) \lambda_{4 \rightarrow 3}^{\psi^+} \psi_{m_1, m_2, m_3-1, m_4+1}^+, \end{aligned} \quad (\text{B4})$$

with initial conditions

$$\psi_{m_1, m_2, m_3, m_4}^-(0) = 0, \quad (\text{B5})$$

$$\psi_{m_1, m_2, m_3, m_4}^+(0) = 0, \quad (\text{B6})$$

$$\phi_{m_1, m_2, m_3, m_4}^-(0) = \begin{cases} p_k (1 - \rho) \binom{k}{m_1} (1 - \rho)^{m_1} \rho^{m_2} & \text{if } m_3 = m_4 = 0, \\ 0 & \text{otherwise,} \end{cases} \quad (\text{B7})$$

$$\phi_{m_1, m_2, m_3, m_4}^+(0) = \begin{cases} p_k \rho \binom{k}{m_1} (1 - \rho)^{m_1} \rho^{m_2} & \text{if } m_3 = m_4 = 0, \\ 0 & \text{otherwise,} \end{cases} \quad (\text{B8})$$

and where  $F$  and  $R$  are defined as

$$F(m_1 + m_3) = \begin{cases} 0 & \text{if } m_1 + m_3 < f, \\ 1 & \text{if } m_1 + m_3 \geq f, \end{cases} \quad (\text{B9})$$

$$R(m_1 + m_3) = \begin{cases} 0 & \text{if } m_1 + m_3 < f, \\ e^{-1/T} & \text{if } m_1 + m_3 \geq f. \end{cases} \quad (\text{B10})$$

- 
- [1] K. Binder and W. Kob, *Glassy Materials and Disordered Solids: An Introduction to Their Statistical Mechanics (Revised Edition)* (World Scientific, Singapore, 2011).
- [2] G. Biroli and J. P. Bouchard, in *Structural Glasses and Supercooled Liquids: Theory, Experiment, and Applications*, edited by P. G. Wolynes and V. Lubchenko (John Wiley & Sons, Inc., Hoboken, NJ, 2012), pp. 31–113.
- [3] L. Berthier and G. Biroli, *Rev. Mod. Phys.* **83**, 587 (2011).
- [4] G. H. Fredrickson and H. C. Andersen, *Phys. Rev. Lett.* **53**, 1244 (1984).
- [5] E. R. Weeks, J. C. Crocker, A. C. Levitt, A. Schofield, and D. A. Weitz, *Science* **287**, 627 (2000).
- [6] W. Götze, *Complex Dynamics of Glass-Forming Liquids: A Mode-Coupling Theory*, International Series of Monographs on Physics (Oxford University Press, Oxford, UK, 2009).
- [7] M. Sellitto, D. De Martino, F. Caccioli, and J. J. Arenzon, *Phys. Rev. Lett.* **105**, 265704 (2010).
- [8] M. Sellitto, *Phys. Rev. E* **86**, 030502(R) (2012).
- [9] D. Cellai and J. P. Gleeson, *Complex Networks IV*, edited by G. Ghoshal, J. Poncela-Casasnovas, and R. Tolksdorf (Springer, Berlin, Heidelberg, 2013), Vol. 476, Chap. 16, pp. 165–172.
- [10] M. Sellitto, *J. Chem. Phys.* **138**, 224507 (2013).
- [11] M. Sellitto, G. Biroli, and C. Toninelli, *Europhys. Lett.* **69**, 496 (2005).
- [12] J. Jäckle and D. Sappelt, *Phys. A (Amsterdam, Neth.)* **192**, 691 (1993).
- [13] S. J. Pitts and H. C. Andersen, *J. Chem. Phys.* **114**, 1101 (2001).
- [14] J. P. Garrahan, R. Jack, V. Lecomte, E. Pitard, K. van Duijvendijk, and F. van Wijland, *Phys. Rev. Lett.* **98**, 195702 (2007).
- [15] F. Ritort and P. Sollich, *Adv. Phys.* **52**, 219 (2003).
- [16] J. P. Gleeson, *Phys. Rev. Lett.* **107**, 068701 (2011).
- [17] J. P. Gleeson, *Phys. Rev. X* **3**, 021004 (2013).
- [18] The transition rates in [17] are actually of the form  $F_{k,m}$ ,  $R_{k,m}$ , where  $k$  is the degree of a node; here we choose to describe them by  $l = k - m$  for the sake of clarity when moving to the description of the four-state dynamics.
- [19] S. N. Dorogovtsev, A. V. Goltsev, and J. F. F. Mendes, *Phys. Rev. Lett.* **96**, 040601 (2006).
- [20] J. Chalupa, P. L. Leath, and G. R. Reich, *J. Phys. C: Solid State Phys.* **12**, L31 (1979).
- [21] D. Cellai, A. Lawlor, K. A. Dawson, and J. P. Gleeson, *Phys. Rev. E* **87**, 022134 (2013).
- [22] Code for all the numerics is available from the authors upon request.
- [23] C. Toninelli and G. Biroli, *J. Stat. Phys.* **126**, 731 (2007).
- [24] A. V. Goltsev, S. N. Dorogovtsev, and J. F. F. Mendes, *Phys. Rev. E* **73**, 056101 (2006).
- [25] M. E. J. Newman, S. H. Strogatz, and D. J. Watts, *Phys. Rev. E* **64**, 026118 (2001).
- [26] H. Silk, G. Demirel, M. Homer, and T. Gross, [arXiv:1302.2743](https://arxiv.org/abs/1302.2743).